THE BIOCLIMATE OF CHOLERA: THE CASE OF HAITI

STEPHEN TENNENBAUM

CAROLINE FREITAG

SVETLANA ROUDENKO

Department of Mathematics, The George Washington University

E-mail addresses: set1@gwu.edu (corresponding author), calliefreitag@gmail.com, roudenko@gwu.edu.

Abstract. We propose a simple model with two infective classes in order to model the cholera epidemic in Haiti. We include the impact of environmental events on the epidemic in the Artibonite and Ouest regions by introducing terms in the force of infection that vary with environmental conditions. We fit the model on weekly data from the beginning of the epidemic until March 2012. We then used this model to obtain epidemic projections from April 2012 through February 2013, and then modified these projections incorporating the vaccination programs that were recently undertaken in the Ouest and Artibonite regions to compare with actual cases.

Using real-time daily rainfall we found lag times between precipitation events and new cases that vary seasonably, ranging from 5 to 11 weeks in Artibonite, and 5.7 to 8.5 in Ouest. In addition, it appears that, in the Ouest region, tidal influences play a significant role in the dynamics of the disease.

Intervention efforts of all types have reduced case numbers in both regions, however, persistent outbreaks continue. In Ouest where the population at risk seem particularly besieged and the overall population is larger, vaccination efforts seem to be taking hold more slowly than in Artibonite where a smaller core population was vaccinated. With the implemented vaccination program the model projects that by the end of February 2013, the number of cases in Artibonite would be decreased by about 7 thousand, and in Ouest by about 3 thousand.

Keywords: cholera, Haiti, bioclimate, epidemic model, vaccination.

1. Introduction

On January 12, 2010, a 7.0 magnitude earthquake struck near Haiti's capital, Port-au-Prince.[1] The poorest nation in the Western Hemisphere, the earthquake shattered Haiti's already weak infrastructure.[1] Thousands of Haitians were killed and even more were forced to flee to resettlement camps.[1]

In October 2010, the first case of cholera was reported in Haiti. A later UN investigation revealed the specific strain of *V. cholerae* came from South Asia.[2] The UN investigation and epidemiological literature suggest that the epidemic began outside of a UN peacekeeper camp near Mirebalais in the Centre department, along the Artibonite River.[2,3] As *V. cholerae* is a waterborne pathogen, the Artibonite River is the ostensible route through which the disease spread throughout Haiti's ten administrative regions, called departments.[4]

Anecdotal news reports describe the dismal situation for thousands of Haitians that still remain displaced months after the earthquake. Sewage of millions of people flow through open ditches. Human waste from septic pits and latrines is dumped into the canals, and after it rains, ends up in the sea. Those living close to the water use over-the-sea toilets, and next to these outhouses, fishing boats unload and sell the fish from plastic buckets...[5]

Haiti's two most populous regions, Ouest and Artibonite, were also the two regions hardest hit by the epidemic. Cases in Ouest and Artibonite account for 60% of the total burden of

cholera in Haiti.[6] For this reason, we chose to focus our analysis on the Ouest and Artibonite regions. By April 7, 2012, cholera had affected 5.7% of the total population* in Ouest and 6.9% of the population in Artibonite.[6]

We reviewed the literature dealing with cholera, modeling, and climatic conditions (rainfall, precipitation, & tides) in Haiti at the beginning of this study and again at the end. We did multi-database searches in the Biology, Medicine, and Health fields and found four modeling papers[7–10] of which the first three used variations of a basic system of differential equations proposed in 2001 by Codeço.[11] At that time, none of these models took environmental conditions directly into account. Two other papers[12,13] have since appeared that do take precipitation into account in cholera. The first[12] is a spatiotemporal Markov chain model using seasonal rainfall which was outside our purview. The second[13] deals specifically with Haiti and was done by the same group that produced one of the earlier papers.[9] Here they looked at the reliability of these earlier studies, and they found that although these models do well in capturing the early dynamics of the epidemic, they fail to track latter recurrences forced by seasonal patterns.[13] As a follow up, Rinaldo et al.[13] add a precipitation forcing function to their original model along with other modifications such as the river network and population mobility. These modifications produce a better fit to the observed pattern of case but predict recurring large outbreaks tracking the seasonal precipitation patterns.

The three models[7–9] proposing a variation on the SIWR model proposed by Codeço in 2001[11] explain cholera transmission through susceptibles' contact with a water reservoir, rather than susceptibles' contact with infectious individuals. The models proposed by Tuite, et al.[8] and Bertuzzo, et al.[9] both incorporated a "gravity" term to study the interaction among regions. The model proposed by Andrews and Basu[7] accounted for a bacterial "hyperinfectivity" stage, following research by Hartley, et al. in 2006 showing that *V. cholerae* initially has a higher infectivity before it decays to a lower infective rate in the aquatic reservoir. The fourth model by Chaoa, et al.[10] was an agent based approach designed to look at various vaccination strategies.

In addition, all these models assessed the impact of potential intervention strategies, including vaccination. Bertuzzo found that a vaccination campaign aiming to vaccinate 150,000 people after January 1, 2011 would have little effect, in part because of the late timing and in part because of the large proportion of *asymptomatic* individuals who would need to get vaccinated.[9] Both the models proposed by Tuite, et al.[8] and Andrews and Basu[7] suggest that vaccination campaigns would have modest effect. In March 2012, Partners in Health began vaccinating 100,000 individuals with Shanchol, a two-dose cholera vaccine.[14] The size of the campaign is limited by the size of the global stockpile of Shanchol.[14] The vaccination campaign is targeted at 50,000 individuals living in the slums of Port-au-Prince, where population density is thought to increase the rate of cholera exposure, and at 50,000 individuals living in the Artibonite River valley, where the epidemic began.[14] Chao et al.[10] showed that

*Note: population data for Haiti is from 2009[4] , one year before the earthquake.

a targeted vaccination strategy would have the best results for this limited supply of vaccine, and by vaccinating 30% of the population the cases could be reduced by as much as 55%.

In 2001, Codeço proposed introducing an oscillating term to model seasonal variability.[11] However, none of the four Haiti-specific models accounted for seasonality. Haiti experienced flooding in June 2011, October 2011, and March 2012.[15] As cholera has reached an endemic state in Haiti, an analysis of cholera's seasonality as it relates to Haiti's rainy season is pertinent. Moreover, mathematical models should incorporate seasonality in order to more accurately predict the course of the epidemic and to simulate the effects of potential interventions. In April 2012 Rinaldo et al.[13] reexamined the above four models (including their own[9]) and concluded that, among other factors, seasonal rainfall patterns were necessary to account for resurgences in the epidemic. They use long-term monthly averages to augment the bacterial growth term of contaminated water-bodies.

Other papers dealing with bio-climate were a study of Cholera in Zanzibar, East Africa that demonstrated 8 weeks fixed delay[16] between rainfall and cholera outbreaks, and another paper in Bangladesh[17] that have a somewhat shorter delay (4 weeks). Both these studies use a statistical approach with seasonal data. Both also made note of the potential influence of ocean environmental factors, and the Reyburn et al. paper included sea surface height and sea surface temperature in their analysis but failed to find any significant relationship.[16] In a third paper Koelle et al. (2005)[18] model very long time periods, more than a year, in Bangladesh. This model also uses seasonal precipitation and models changes in the susceptible fraction of the population due to demographics and loss of immunity.

In this paper we use detailed and current rainfall, temperature, and tidal records to model cholera in the Artibonite and Ouest regions. We forego a bacterial compartment in favor of an *a posteriori* approach using climatic data directly to estimate infection rates. This has the advantage of more tractable temporal estimates without over parameterizing and including compartments that are essentially unmeasurable. This paper is also the first, that we know of, that uses tidal variation in a model of cholera dynamics.

These long term trends and environmental influences established the pattern of response of the epidemic in Artibonite and Ouest. Thus parameters were chosen and model calibration set prior to a vaccination program being implemented. We then used the model to evaluate the performance of the vaccination program against the backdrop of an alternative history without vaccination.

2. Material and Methods

For Ouest and Artibonite, we investigated the correlations between reported cholera cases and rainfall, temperature, and in the case of Ouest, tidal range. We wanted to determine a) if such correlations exist, b) the time delay between environmental conditions and recorded cholera outbreaks, and c) if effectiveness of a recent vaccination program could be assessed by use of this model.

2.1. **Model.** We take a combined mechanistic and phenomenological approach to our model. The mechanistic part is a standard SIR type model where individuals move from *Susceptible* (S) to *Infected* to *Recovered* (R) classes*. An infectious individual may either be *symptomatic* (I) or *asymptomatic* (A).[20] The probability, ρ, of asymptomatic infection is 0.79.[20,21] Both *symptomatic* and *asymptomatic* individuals move to the recovered group, R, at a rate γ. *Symptomatic* individuals die from cholera at a rate μ (dead are denoted by D).

The phenomenological part comes from estimating the force of infection, $\beta(t)$, by fitting the number of cases predicted by the model (both incidence and cumulative cases) to the data. This has the benefit and drawback of eliminating the connection, *in the model*, between the infected population and the infecting water bodies, food, and so on. A benefit since we don't need to model and estimate the extra compartments and half dozen or so other parameters necessary to incorporate the mechanism of environmental bacterial populations and their containing water bodies. And a drawback because an important mechanism is no longer included in the model. We are obviously not suggesting that such feedbacks don't exist, only that they are beyond the scope of this study. All other parameters are discussed below and values are given in Table 1 and Table 2.

This paper evaluates Artibonite and Ouest separately, in order to capture the varying dynamics in each region. We use the following system of ordinary differential equations, and the components to be fitted: $N = S + A + I + R + D$, where N is the initial population of the region. (For the purposes, and time scale, of this study we chose to ignore the demographics of the population.)

System of equations $\qquad\qquad$ Variables to be fitted

$$\left\{ \begin{array}{l} \frac{dS}{dt} = -\beta(t)\, S \\ \frac{dA}{dt} = \rho\beta(t)\, S - \gamma A \\ \frac{dI}{dt} = (1-\rho)\beta(t)\, S - (\gamma+\mu) I \\ \frac{dR}{dt} = \gamma(A+I) \end{array} \right\} \implies \left\{ \begin{array}{l} \text{new cases} = (1-\rho)\int_{t-\Delta t}^{t} \beta(\xi)\, S(\xi)\, d\xi \\ \text{total cases} = (1-\rho)\int_{0}^{t} \beta(\xi)\, S(\xi)\, d\xi \end{array} \right\}$$

2.2. **Environmental Effects.** We assume that significant rain events will cause flooding, which will increase direct contact the bacteria via contaminated water, or indirectly via soils, vegetation, and disease bearing insects, etc. that have been contaminated or consumed cholera bacteria. We also assume that temperature plays a dual role by increasing the infection rate and decreasing the lag time between rainfall events and disease outbreaks.

Additionally, in the Ouest region there are commercial areas, tent-cities and slums that have raw waste directly discharging to Port-au-Prince Bay, or to the bay via rivers (e.g. Froide, Momance, and Grise), and numerous open sewage canals. We hypothesis that there may be additional disease generated when large tidal ranges stir up contaminated sediments or cause

*Conceptually the underlying model is a variation on the SIWR model, which assumes that cholera is spread through susceptibles' contact with contaminated water, food or fomites. This model uses the amount of water consumed as a proxy for all possible modes of transmission, and the concentration of bacteria in the water consumed modifies the infection rate by a dose-response expression (see[19] with a base model[11])

blooms of plankton in these coastal waters. Again the chain of infection may be complex and include direct contact with water, insects, or consumption of contaminated seafood, etc.

Therefore, we modify the force of infection term, β, such that

$$\beta(t) = u(t)\left[\alpha_p H(t)\, P(t-\tau_p,\theta_p) + \alpha_m M(t-\tau_m,\theta_m)\right], \tag{1}$$

where P is a moving average of the amount of daily rainfall, and M is a moving average of the maximum semi-diurnal tidal range, H is a heat index based on mean air temperature, τ_p, is the lag time for precipitation (which is itself affected by temperature), τ_m is the lag time for tides, θ_p, and θ_m are the averaging periods, and α_p, and α_m are proportionality constants.

We also included an expression for improvement of conditions over time, either through reducing the effective susceptibles, or reduction in the infection rate, or both. These factors would be due to increased access to clean water, increased personal hygiene, decreased contamination of the environment, vaccination, and rapid treatment of new cases, or any other means of removing risk. We assume the force of infection is reduced by an exponential decreasing factor $u(t) = e^{-rt} + (1 - e^{-rt})u_0$, where r is the rate of improvement in conditions and $1 - u_0$ is the maximum amount of improvement possible in the short term (u_0 can be considered the persistent fraction of risk remaining in a region). This approach is tantamount to having the susceptible, or at-risk population reduced directly by public health improvements[†].

2.3. **Data.** The source of the epidemic data was *the Haitian Ministry of Public Health and Population* and compiled by *the Pan American Health Organization*.[4,6] The data sets available, which we used for this study, consist of cumulative cholera cases, and new cholera cases. New cholera cases are calculated based on the difference between the latest report and the previous one. Cholera case definition also includes suspected cholera cases and deaths in addition to confirmed cases and deaths. As such, data posted on the web site are periodically updated with minor corrections. Cases are reported on weekly basis with the reporting week beginning on Sunday.

Reported hospitalized cases and hospitalized deaths are probably more accurate, but for the purposes of this study, less useful, since we want to track the progress of the epidemic, and increases in *access* to treatment biases the data. New case estimates for the first few weeks of the epidemic are unavailable. Total cases (TC) for the first 4 weeks was obtained by regressing, for the following 8 weeks (14-Nov-10 through 2-Jan-11), the reported total cases against hospitalized cases (HC). For the Ouest region $TC_O = 2.2HC_O$ $(R^2 = 0.99)$, and for the Artibonite region $TC_A = 2.59HC_A + 497$ $(R^2 = 1.00)$.

Rainfall, temperature and tide data were compared to the pattern of new cholera cases reported each week. The rainfall data comes from NASA,[22] using centrally located points in each region as our datum point, given by (latitude, longitude). For Artibonite our datum point is $(19.125, -72.625)$ and for Ouest, it is $(18.625, -72 \cdot 375)$.[22] NASA updated

[†]For example $\beta(t) = \alpha_p H(t)\, P(t-\tau_p,\theta_p) + \alpha_m M(t-\tau_m,\theta_m)$, $\frac{dS}{dt} = -\beta(t)\, S - r\left(1 - \frac{u_0}{u}\right) S$, and $\frac{du}{dt} = -r\,(u - u_0)$, etc. Where the rate of reduction of risk of the susceptible population starts at $r\,(1 - u_0)$ and decreases to 0 when $u = u_0$.

its processing of the data during the course of this project from TRMM_3B42_daily.006 to TRMM_3B42_daily.007. Although our initial investigation used the version 6 material, all figures and parameter estimates given in this paper are using version 7. Precipitation estimates are a combination of remote sensing and ground verified information reported with a spatial resolution of 0.25×0.25 degrees and a temporal resolution of 1 day, further details are available on the web site.[22]

Temperature data is mean daily air temperature at Port-au-Prince, and is reported by the Weather Underground.[23] Although we had daily numbers for Temperature we chose to extract the annual cycle and use that in simulations. This has the advantage of allowing us to extrapolate temperature for model projections.

Tide data is for Port-au-Prince Bay (StationId: TEC4709).[24] These numbers are predictions from NOAA's tide model for this location and are not direct measurements. NOAA's web site allows you to download tide numbers for any date starting from 2010 and extending through 2014.

The initial modeling was done by comparing data sets in the frequency domain for new cases and rainfall in order to find any suggestions of matching periodicity and/or time-lags. Code was then written in Berkeley Madonna to simulate the dynamical system, and try various manipulations of the environmental data in order to match predictions to data[‡]. Rainfall data was available only to week of 30-Sept-2012 (week 102) because of the lag between the timing of rainfall events and what had been processed at the time we accessed it.[22]

2.4. **Model calibration.** All modeling and calibration was done in Berkeley Madonna. When possible we used reasonable ranges for each parameter as established by previously published research (see Table 2). Since our model contains several fitted parameters, we attempted to minimize the plausible range for each parameter in order to obtain a more accurate fit. Parameter values not obtained from the literature were adjusted in an iterative fashion to narrow their initial ranges, fitting by eye predicted number of new cases to the reported number of new cases. The Berkeley Madonna curve fitting algorithm was then used to minimize the root mean square difference between model predictions of number of cumulative cases and reported cases for the restricted parameter space. Confidence and prediction intervals were calculated using the delta method.[25]

2.5. **Parameters from literature.** Table 1 displays parameter values for each region obtained from published or online sources.

2.6. **Environmental components of the force of infection.**

[‡]When we discuss the output of our model, will use the term "prediction" to indicate the numbers generated during the calibration phase of the model and "projection" to indicate the extrapolation of the model past cases used for the calibration.

Parameter	Artibonite	Ouest	Units or calculation	References
ρ	0.79	0.79	fraction becoming asymptomatic	[20, 26]
γ	1.4	1.4	fraction recovered per week	[7, 9, 11]
N_0	1,571,020	3,664,620	–	[4]
S_0	1,534,338	3,663,699	$N-(A_0+I_0+R_0+D_0)$	
I_0	7,653	193	regression on early hospitalized cases	[6]
A_0	28,790	726	$\frac{\rho}{1-\rho}I_0$	
R_0	0	0	–	
D_0	239	2	–	[6]
t_0	17-Oct.-2010	17-Oct.-2010	290^{th}day of the year	[6]
u_0	0.05	0.05	persistant fraction of pop. at risk	[27]

TABLE 1. Parameter values obtained from literature.

2.6.1. *Artibonite.* Bioclimatic influences on infection rate are a product of precipitation rate and an heat index. Daily precipitation $p\,(t)$[22] is averaged over an interval θ_p so the running average precipitation rate is

$$P(t-\tau_p,\theta_p)=\frac{1}{\theta_p}\sum_{j=0}^{\theta_p}p\,(t-\tau_p-j)\,,$$

where τ_p is the delay in precipitation's affect on infection rate (see below). For the delay we used a simple sine function to model a mean temperature index throughout the year. (Temperature data from.[23]) The mean air temperature index given by

$$T_{air}\,(t)=\sin\left(\frac{2\pi\,(7t+187)}{365.25}\right),\qquad \text{where } t \text{ is in weeks from 17-Oct.-2010.}$$

This is then used to create a delay functions that varies from a minimum of τ_{p_lo} during summer and τ_{p_hi} during winter

$$\tau_p=\left(\left(\tau_{p\_hi}+\tau_{p\_lo}\right)-\left(\tau_{p\_hi}-\tau_{p\_lo}\right)T_{air}\,(t)\right)/2.$$

In other words, infections result faster in the summer than in the winter months. This would be expected since warmer temperatures mean faster growth rates for bacteria and their invertebrate hosts as well as triggering emergence of spores.[17, 28]

In addition, there is a direct influence of temperature on the infection rate. This heat index is given by

$$H\,(t)=1+kT_{air}\,(t)\,.$$

Finally, the infection rate is given by

$$\beta\,(t)=u(t)\,\alpha_p H(t)\,P(t-\tau_p,\theta_p)\,.$$

2.6.2. *Ouest.* For the Ouest region we use the same formulation as in Artibonite, however, we found that tidal *range* appeared to significantly affect infection rates as well. The maximum tidal range each day (there are two) $m\,(t)^{24}$ is averaged over an interval θ_m so the running average precipitation rate is

$$M(t-\tau_m,\theta_m)=\frac{1}{\theta_m}\sum_{j=0}^{\theta_m} m\,(t-\tau_m-j)-M_0,$$

where τ_m is the delay in the tide's affect on infection rate. Here, τ_m is fixed, the effect of temperature (water or air) on lengthening or shortening the response in infection rate was not found to be sufficient to warrant adding another function and additional parameters. Thus, the overall infection rate for Ouest is

$$\beta\,(t)=u(t)\left[\alpha_p H(t)\,P(t-\tau_p,\theta_p)+\alpha_m M(t-\tau_m,\theta_m)\right].$$

3. RESULTS

3.1. **Parameter Fitting and Model Selection.** The following Table 2 displays parameter values for each region obtained through curve-fitting to cumulative reported cases.

parameter	Artibonite	Ouest	units	description
θ_p	4.61 (0.319)	1.96 (0.526)	weeks	averaging window for precip.
τ_{p_lo}	0.4019 (0.3261)	3.800 (0.3757)	weeks	minimum delay for precip. effects
τ_{p_hi}	7.1805 (0.2056)	6.500 (0.4240)	weeks	maximum delay for precip. effects
k	0.5198 (0.0177)	0.5812 (0.03050)	$^\circ\mathrm{C}^{-1}$	temp.-precip. interaction level
α_p	$6.8806\ (0.1690)\times10^{-3}$	$1.1502\ (0.08582)\times10^{-3}$	$(\text{mm}\times\text{week})^{-1}$	infection rate per mm rain
θ_m	–	1.00 (0.91)	weeks	averaging window for tidal range
τ_m	–	1.960 (0.494)	weeks	delay for tidal range effects
α_m	–	$2.8128\ (1.3360)\times10^{-4}$	$(\text{cm}\times\text{week})^{-1}$	infection rate per cm tide range
M_0	–	24.791 (24.094)	cm	baseline of tidal range effect
r	0.06100 (0.00147)	0.02610 (0.00139)	week^{-1}	decrease in susceptibles per week

TABLE 2. Parameter values obtained from model calibration. Numbers in parentheses are 95% confidence intervals (CI's).

After initially restricting the parameter search space by visually fitting the New Cases predicted to the New Cases data, we used the Berkeley-Madonna curve-fitting routine on cumulative cases and in an iterative fashion. We first optimized the averaging windows (θ's) and delays (τ's), then temperature interaction level (k), infection rates (α's), and the improvement rate (r). We then re-optimized the averaging windows and delays and then a final fit for the parameters α_p, r and for Ouest α_m. This was done for two reasons, first, the high variability of the data and the non-linearities of the averaging windows and delays lead to a number of local minima of the RMSD's, and second we wanted to search in a particular basin that corresponded to our visual fit of the New Cases. Allowing the software to search

the entire parameter space all at once would inevitability cause it to jump from basin to basin to find a global minimum for *just* cumulative cases.

The Artibonite model *with* tide was not included in Table 2 since inclusion of tide did not improve the model (see Tables 3 and 4). The statistics for the model fit are given in the following two tables. Table 3 is for cumulative cases predicted by the model compared to cumulative case data.

All cases				
statistic	Artibonite (tide)	Artibonite (no tide)	Ouest (tide)	Ouest (no tide)
data points	77	77	74	74
parameters	10	6	10	6
adj RMSD	2181.40	2121.78	3708.59	6336.53
adj R^2	0.9930	0.9933	0.9968	0.9908
AIC	1193.20	1185.40	1271.40	1352.56

TABLE 3. Model predictions versus data statistics for *cumulative number of cases*: Root mean squared deviations (RMSD), Coefficient of determination (R^2), and Akaike information criterion (AIC). Degrees of freedom for the statistics are adjusted by the number of parameters fit in the calibration process.

For the full model in either region (model including tides) the parameters θ_m, τ_m, M_0, and α_m are added and the model is re-optimized. For Artibonite an F-test for the nested models gives the following results $F = 0.043$ $d.f. = (4, 67)$ and the p value is 0.9964, indicating the inclusion of the extra detail had almost no effect and would be unjustified. For the Ouest region an F-test for the nested models gives the following results $F = 33.63$ $d.f. = (4, 64)$ and the p value is 4.208×10^{-15}, indicating the tidal data significantly improved the model fit.

New cases				
statistic	Artibonite (tide)	Artibonite (no tide)	Ouest (tide)	Ouest (no tide)
data points	77	77	74	74
parameters	10	6	10	6
adj RMSD	9.601	9.348	21.30	23.08
adj R^2	0.7913	0.8027	0.3932	0.3681
AIC	357.62	349.97	461.92	470.28

TABLE 4. Model predictions versus data statistics for *new cases*: Root mean squared deviations (RMSD), Coefficient of determination (R^2), and Akaike information criterion (AIC). Degrees of freedom for the statistics are adjusted by the number of parameters fit in the calibration process.

Table 4 is for new cases predicted by the model compared to new case data. The statistics in Table 4 are done on the square roots of the values in order to produce more uniformly distributed data and stabilize the variance somewhat. The F-test for the Artibonite nested models using new cases gives the following results $F = 0.0755$ $d.f. = (4, 67)$ and the p value is 0.9894. For Ouest the difference is again highly significant with $F = 3.9599$ $d.f. = (4, 64)$ and the p value is 0.0062.

3.2. **Lag times.** The total delays in response to precipitation and tides are the sum of the averaging window and the delay function. For precipitation the minimum and maximum delays for Artibonite are 5.0 and 11.8 weeks, and for Ouest they are 5.7 and 8.5 weeks, respectively. The shorter delays are very similar in the two regions during the warmer months but during the cooler months the response time in Artibonite is 3 weeks longer. These long delays are similar in magnitude to delays reported from a study of Cholera in Zanzibar, East Africa (8 weeks fixed delay),[16] and the shorter delays (4 weeks) to those in Bangladesh.[17] For Ouest estimated delay from response to changes from tidal range was about 3 weeks. But since influence of tidal range has not been quantitatively reported elsewhere in the literature, we have nothing to compare this number to.

Although, rainfall data was available only to week of 26-Feb-2012 (week 71), we run the simulations for another month, until 1-Apr-2012 (1st day of week 76), just short of the minimum time lag between precipitation events and new cases.

3.3. **Vaccination.** A program to vaccinate *the most at risk populations* began in the 2nd week of April and ended in mid June. Each site (Ouest and Artibonite Dept) vaccinated about 50,000 persons, and each site had about 91% 2nd dose coverage. The administration of the first dose was staggered by age groups (beginning first with 10 year olds and up) because the Ministry of Health had a measles, rubella and polio vaccine catch-up campaign for children under 10 years of age that was taking place at the same time last April 2012.[§]

In the Ouest Department, GHESKIO vaccinated adults, adolescents and children over 10 years of age from April 12-23, 2012 and children under 10 from May 26 - June 3. Vaccine was provided to 99,877 persons (52,357 with the first dose, and 47,520 the second dose) living in the slums of Port-au-Prince and surrounding villages.[¶]

In the Artibonite Department, PIH vaccinated 32183 people in rural Bocozel and 13185 people in Grand Saline with 90.8% of those people confirmed to get the 2nd dose (or 41194 for both locations). The campaign started April 15th 2012 and ran until June 10 2012. Here too, children under 9 year old were vaccinated in the second half of the time period because of the MMR and Polio vaccination campaign.[‖]

With these basic facts we constructed a crude vaccination schedule (Table 5) using the following assumptions:

[§]Communicated by Jordan Tappero, MD, MPH (CDC/CGH/DGDDER, Atlanta, GA). Nov. 29, 2012.

[¶]Communicated by Jean W. Pape, MD (GHESKIO, Weill Cornell Medical College, Port-au-Prince, Haiti). Nov. 29, 2012.

[‖]Communicated by Louise Ivers, MD (Partners in Health/ZL, Cange, Haiti). Nov. 29, 2012.

1) approximately 25% of the population is under 10 years old;
2) the second dose was administered 14 days after the first dose was given;[29]
3) the immune response took hold about 8.5 days after the second dose was given;[29]
4) we used the average number of people vaccinated per day over a 12 day period for adults and 9 days for children.

Ouest		
Adult 1^{st} dose	$39,268$	April 10 - April 23
Adult 2^{st} dose	$35,640$	April 26 - May 7
Adult immune response	$65-85\%$	May 4 - May 15
Child 1^{st} dose	$13,089$	May 26 - June 3
Child 2^{st} dose	$11,880$	June 9 - June 17
Child immune response	$65-85\%$	June 17 - June 25
Artibonite		
Adult 1^{st} dose	$34,026$	April 15 - April 26
Adult 2^{st} dose	$30,896$	April 29 - May 10
Adult immune response	$65-85\%$	May 7 - May 18
Child 1^{st} dose	$11,342$	May 19 - May 27
Child 2^{st} dose	$10,298$	June 2 - June 10
Child immune response	$65-85\%$	June 10 - June 18

TABLE 5. Simulated vaccination schedule for Artibonite and Ouest

We ran simulations including vaccination by removing, in Artibonite, 2574.67 at risk persons over age 10 per day starting on 7-May-2012 and ending on 18-May-2012 (30896 total), then removing 1144.22 at risk children per day starting on 10-June-2012 and ending on 18-June-2012 (10298 total). In Ouest we removed, 2970 at risk persons over age 10 per day starting on 4-May-2012 and ending on 15-May-2012 (35640 total), then removing 1320 at risk children per day starting on 17-June-2012 and ending on 25-June-2012 (11880 total).

Since the efficacy of the vaccine (oral Shanchol) is between 65 and 85%[29] we did three runs $65, 75, \text{and} 85\%$ for each department. The 75% run was our mean. To get the bounds we added the 95% prediction interval to the 65% run and subtracted it from the 85% run.

3.4. **Simulations and Projections.**

3.4.1. *Predictions compared to observations for cumulative and new cases.* The following Figures 1 and 2 show the model predictions compared to observations for cumulative number of cases in Artibonite and Ouest regions, respectively. Similarly Figures 3 and 4 show the model predictions compared to observations for new number of cases in Artibonite and Ouest regions, respectively. Prediction intervals were calculated only for the cumulative numbers

since the final model fitting was done on these numbers. Confidence intervals are shown for incidence. The match for the trends in new cases match fairly well, the slope of the expected (model) regressed against observed (data) is nearly one in both departments (see Figures 5 and 6) even though there is a substantial amount of unexplained variance. Whether this is due to the crude spatial resolution or other factors remains to be seen.

Prediction intervals (PI's) and confidence intervals (CI's) were calculated using the delta method adapted for differential equations (see, for example, Ramsay et al.[25]). After 30-Sept-2012 rainfall data from NASA was unavailable, for simulations after that date we did 13 runs using rainfall patterns from each of the 13 prior years. The mean of those simulations was used and the variance of the 13 runs, at each time step, was added to the variance from the estimation procedure before computing the PI's.

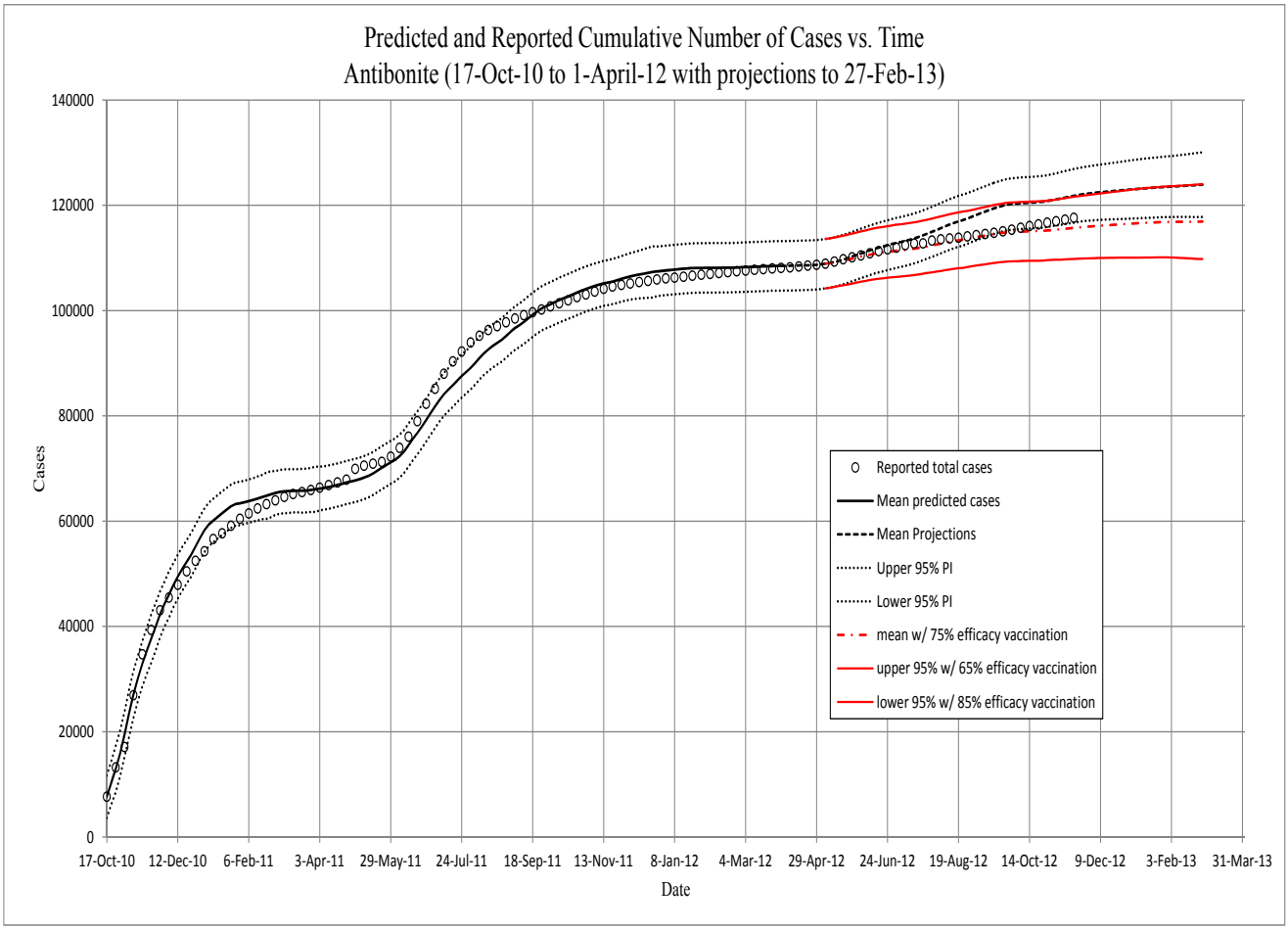

FIGURE 1. Artibonite. The predicted cumulative number of *symptomatic* individuals, against total reported cases to 1-Apr-2012. Projections are from then to end of February. Projections using the vaccination schedule (red) begin on 7-May-2012, approximately three weeks after beginning the vaccination program in Artibonite. All projections after 11-Nov-2012 are based on runs using prior 13 years of precipitation, and PI's include the variance of those data (see text).

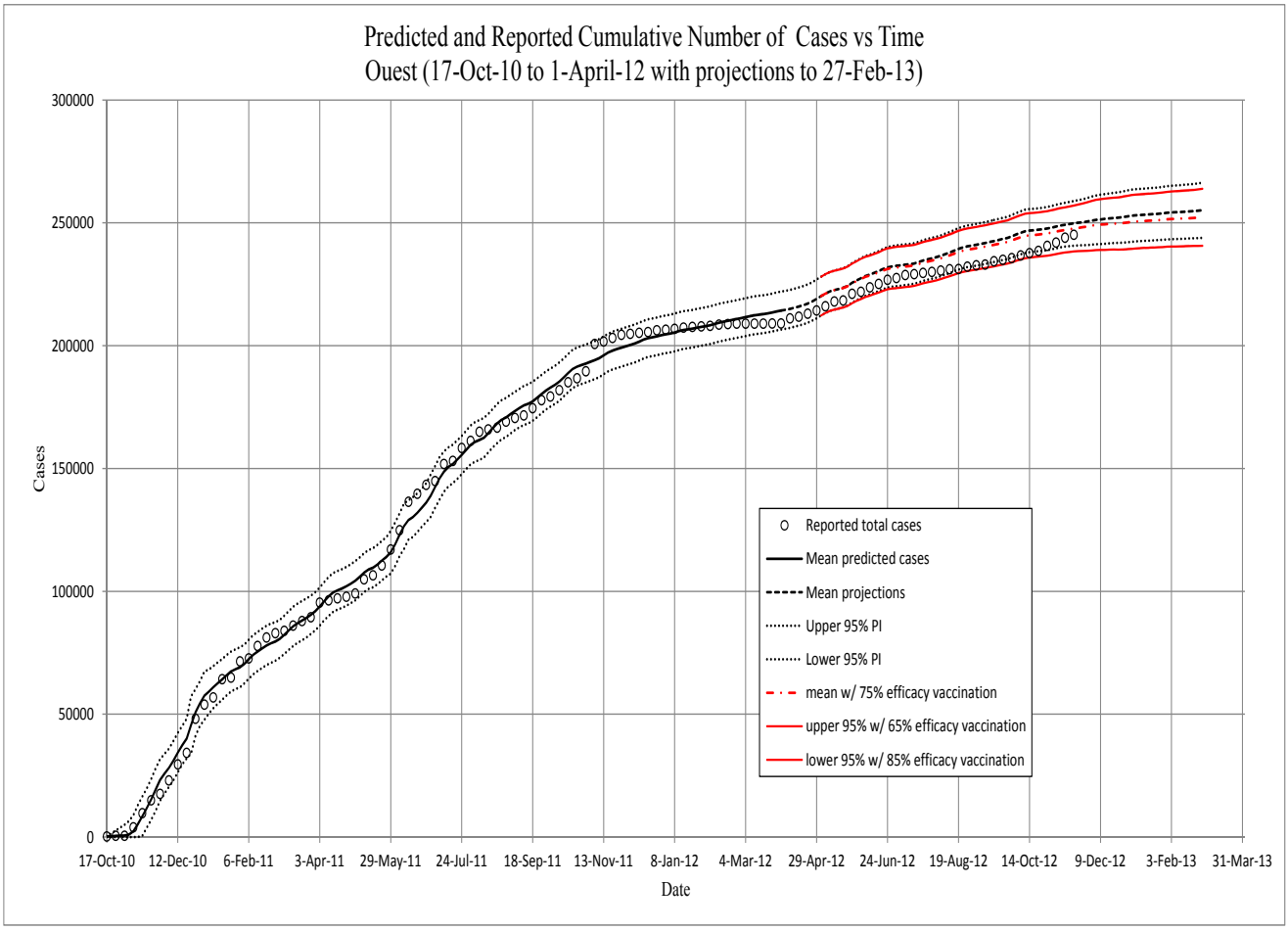

FIGURE 2. Ouest. The predicted cumulative number of *symptomatic* individuals, against total reported cases to 1-Apr-2012. Projections are from then to end of February. Projections using the vaccination schedule (red) begin on 4-May-2012, approximately three weeks after beginning the vaccination program in Ouest. All projections after 11-Nov-2012 are based on runs using prior 13 years of precipitation, and PI's include the variance of those data (see text). Note that for the Ouest region, the model begins at the *fourth week*. We assume that the low initial numbers in the first three weeks are a result of immigration of cases from the Artibonite region. The model therefore uses data for the first four weeks – assumed immigration numbers for the first three weeks and the initialization of the model from data for the fourth week.

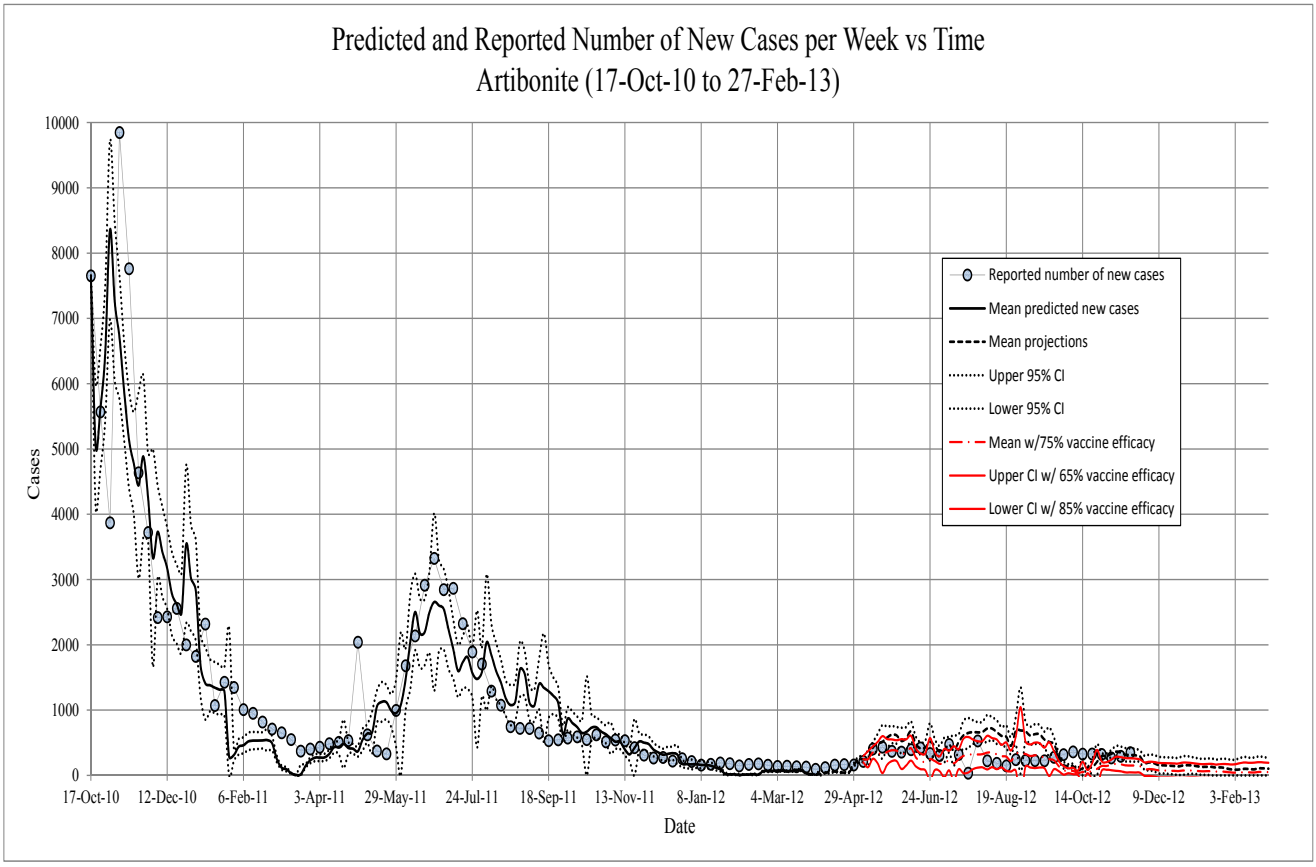

FIGURE 3. Artibonite. The new *symptomatic* individuals, vs. time. Circles - observed; solid line - model prediction; Dashed lines - 95 percentile confidence intervals for model projections. Red line is projections with 75 percent vaccine efficacy.

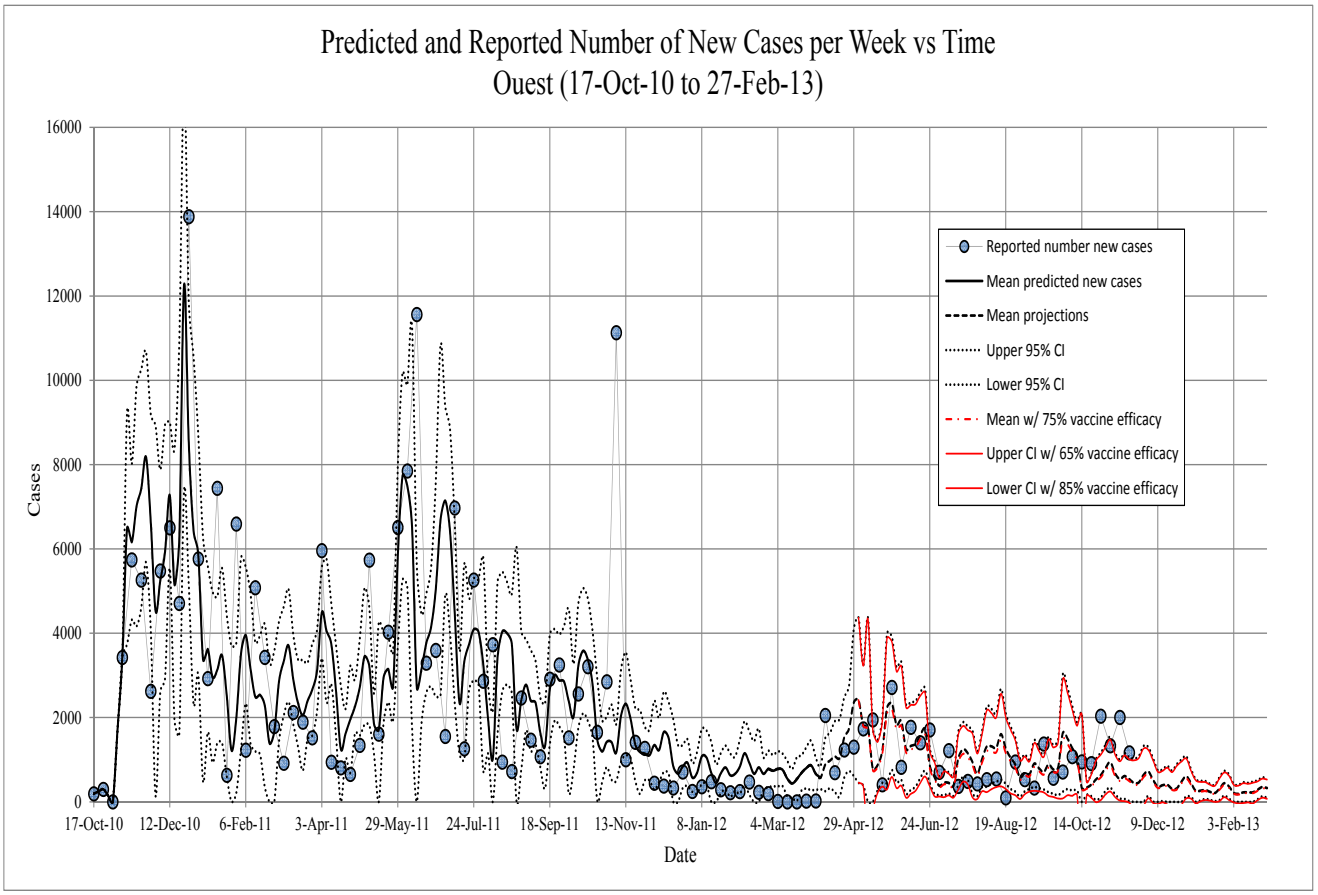

FIGURE 4. Ouest. The new *symptomatic* individuals, vs. time. Circles - observed; solid line - model prediction; Dashed lines - 5, 50, and 95 percentiles for model projections based on past 13 years precipitation records.

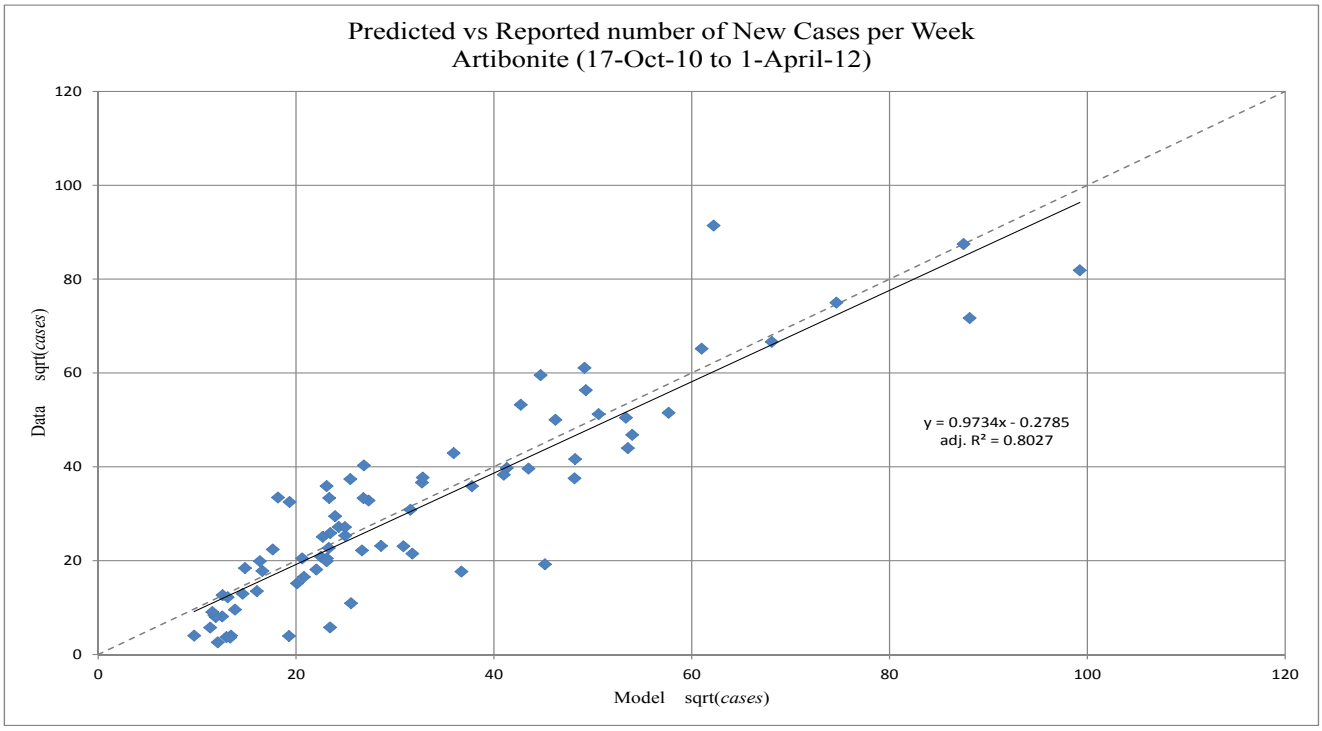

FIGURE 5. Artibonite. The predicted new *symptomatic* individuals, against weekly reported cases to 1-Apr-2012 (square root transformed). A regression line matching the main diagonal (45°) dashed line would show an optimal fit, the discrepancy is due in part to fitting on the cumulative numbers.

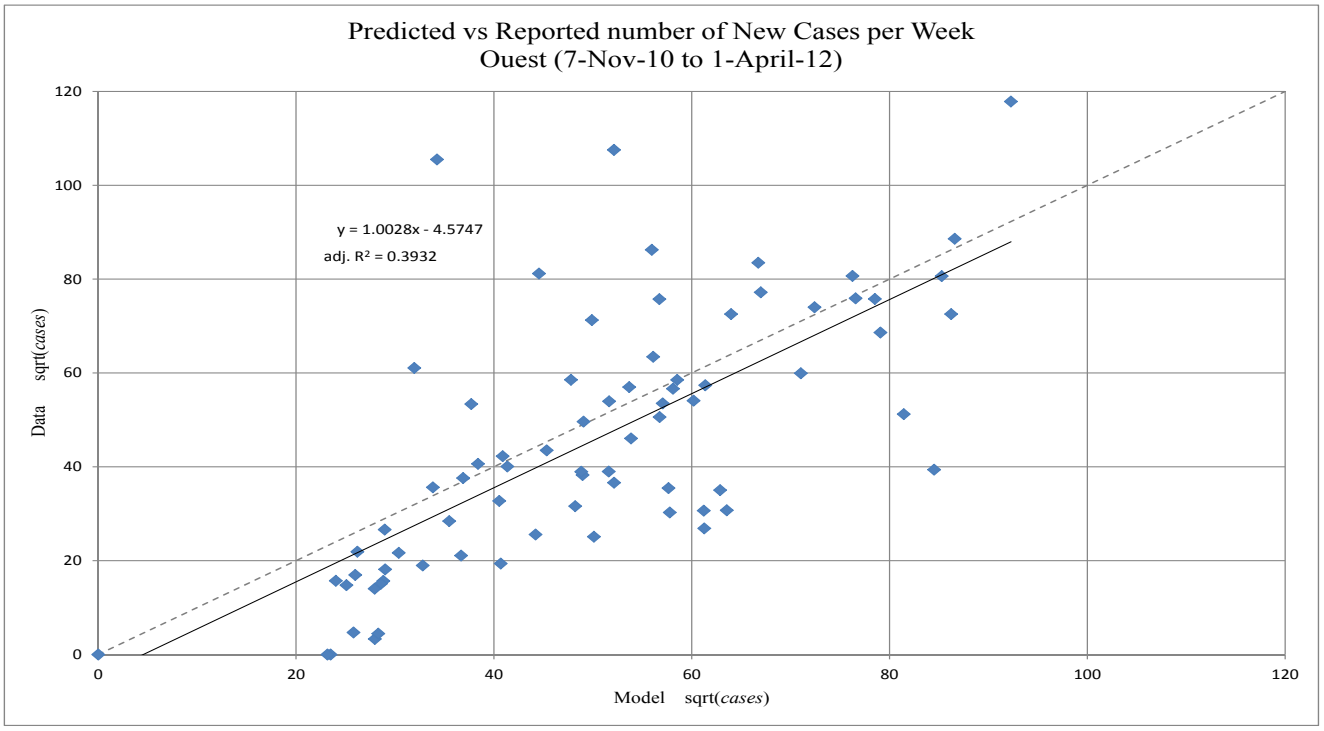

FIGURE 6. Ouest. The predicted new *symptomatic* individuals, against weekly reported cases to 1-Apr-2012 (square root transformed). A regression line matching the 45° line would show an optimal fit, the discrepancy is due in part to fitting on the cumulative numbers.

3.4.2. *Epidemic projections for Artibonite.* The model projects that by the end of February 2013, Artibonite would have seen between 117 and 130 thousand cholera cases without vaccine, and between 110 and 124 thousand with the implemented vaccination program (a decrease in about 7 thousand cases; see Figure 7). The model also predicted that about 15002 people would have gotten ill between the onset of the immune response (6-May) and the end of the simulation (27-Feb) this represents about a 47% decrease in the number of people that would have gotten cholera. The F value comparing the mean values of two models to the actual cases between 6-May and 2-Dec is 9.88 with 25 degrees of freedom for both models, yields a p-value of 1.06×10^{-7}. This suggests that the different models (with and without vaccination) show a substantial difference in how well they match cumulative number of cases data. There seems to be better agreement between the projected and observed incidence as well (see Figure 8) where the number of new cases is well below what would have occurred without vaccination.

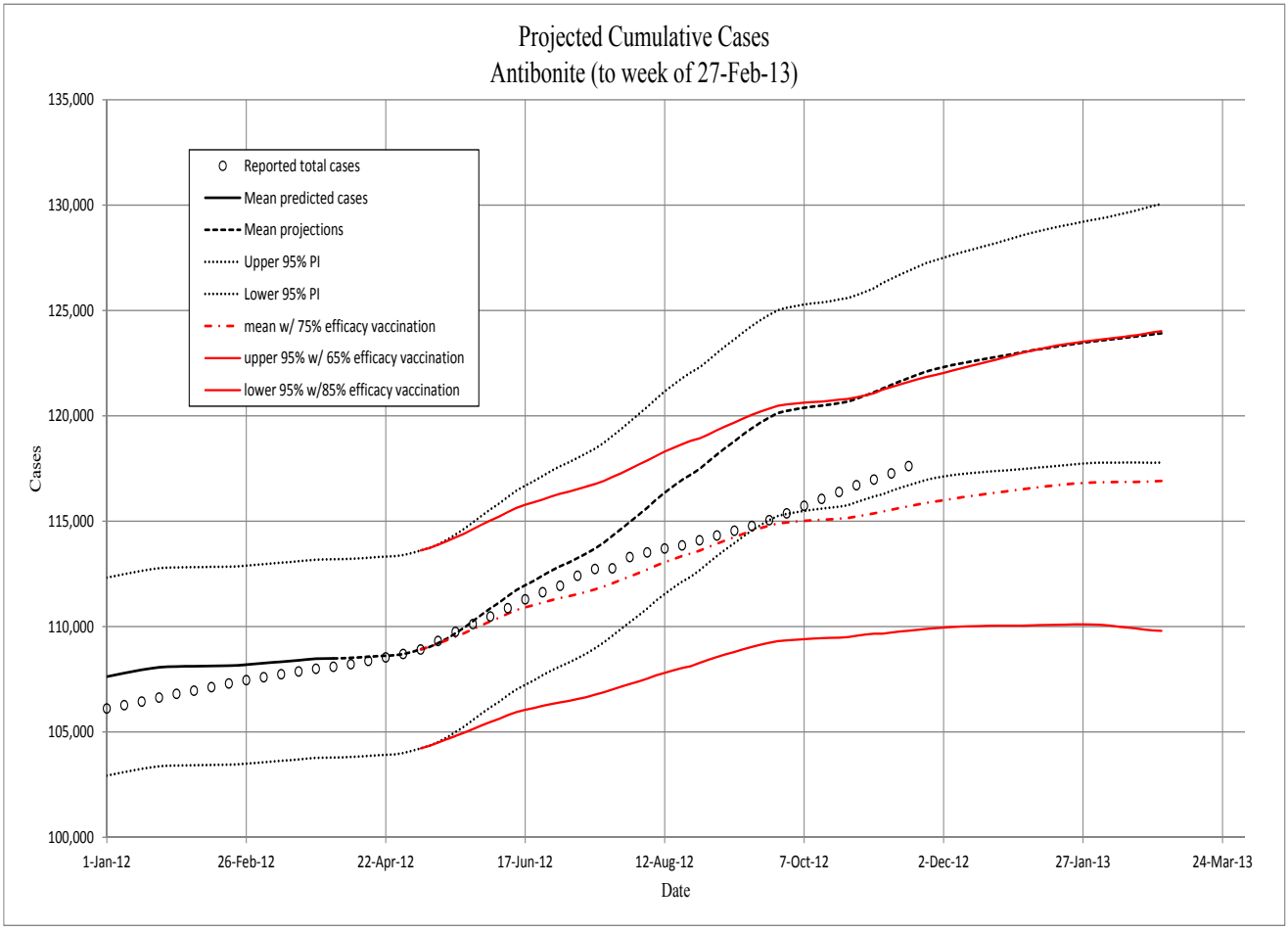

FIGURE 7. Artibonite. The projected total *symptomatic* individuals, vs. time. Circles - observed; solid line - model prediction; Dashed lines - 5, 50, and 95 percentiles for model projections based on past 13 years precipitation records. Red lines are model runs with vaccination schedule that occurred in Spring 2012 (see text).

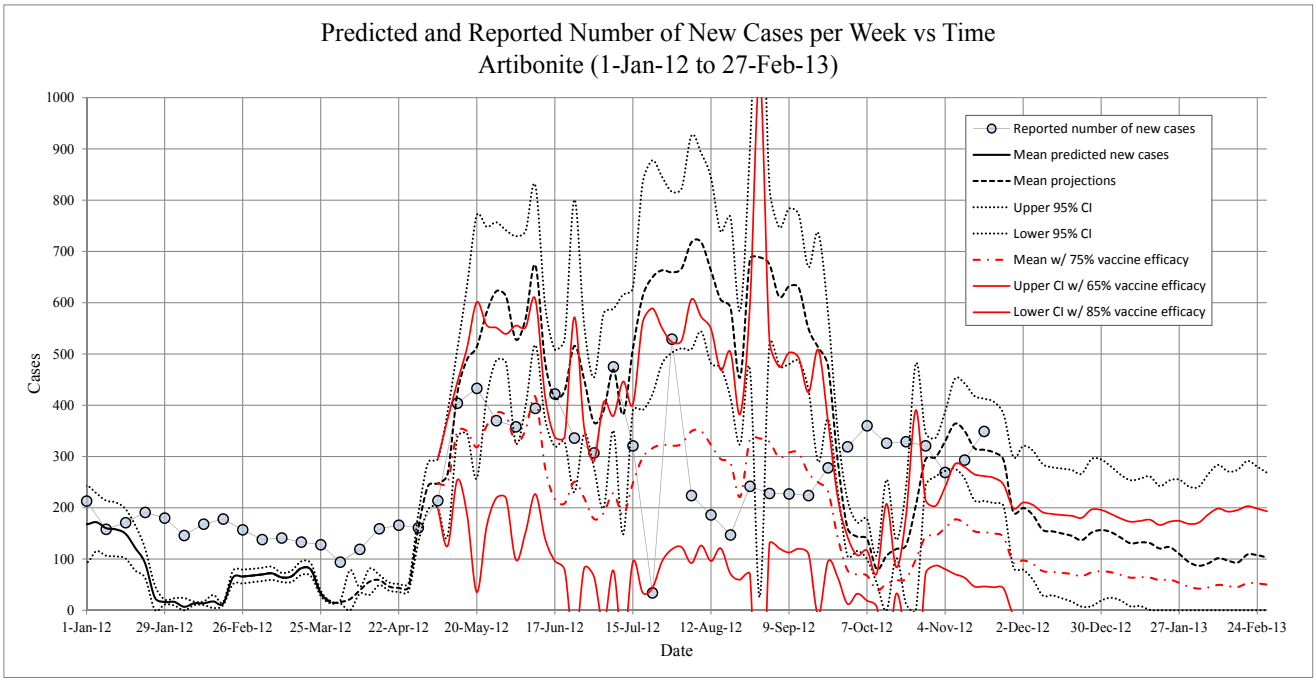

FIGURE 8. Artibonite. The projected new *symptomatic* individuals, vs. time. Circles - observed; solid line - model prediction; Dashed lines - 95 percentile confidence intervals for model projections. Red line is projections with 75 percent vaccine efficacy.

3.4.3. *Epidemic projections for Ouest.* For Ouest, the model projects that by the end of February 2013, Ouest would have seen between 244 and 266 thousand cholera cases without vaccine, and between 241 and 264 thousand with the implemented vaccination program (a decrease in about 3 thousand cases; see Figure 9). The model also predicted that about 33909 people would have gotten ill between the onset of the immune response (6-May) and the end of the simulation (27-Feb) this represents about a 8.4% decrease in the number of people that would have gotten cholera. The F value comparing the mean values of two models to the actual cases between 6-May and 2-Dec is 1.47 with 21 degrees of freedom for both models, yields a p-value of 0.17. This suggests that the different models (with and without vaccination) do not substantially differ in how well they match cumulative number of cases data. Note that this *does not mean* that the vaccination program did not have an impact, but only that the model at this point in time could not distinguish between a scenario with and without vaccination. There was a slowdown in number of new cases in starting in mid February and running through March which dropped the cumulative case number below the mean model projections (but still within the prediction interval), however, this occurred *before* the vaccination program took place. There was another smaller slowdown in July but this was being made up for by a rapid growth in numbers in November (see Figure 9). It would seem that these oscillations are in spite of, rather than because of vaccination, since the model predicts a steady, albeit slow, additional decline in new cases(see Figure 10).

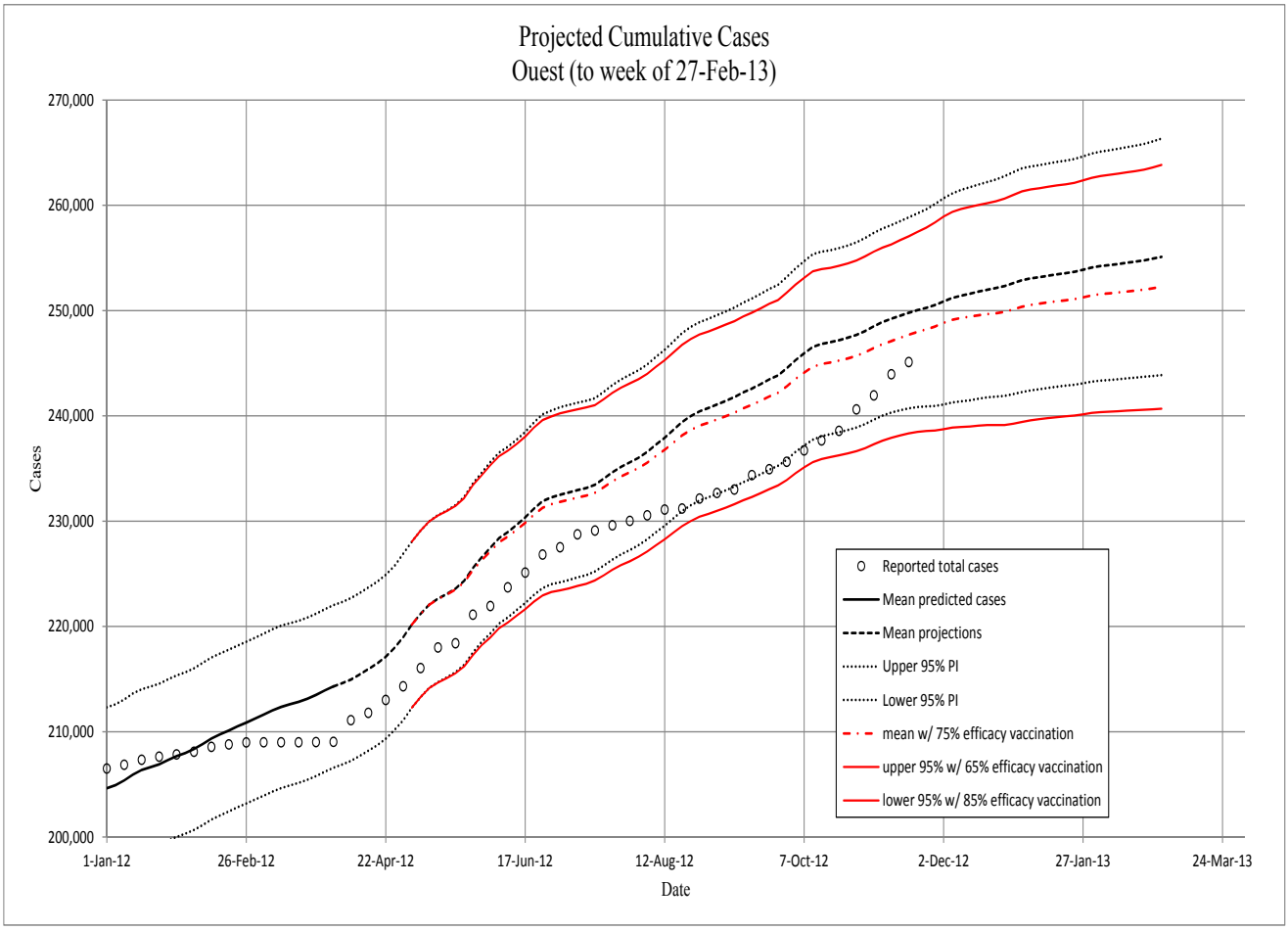

FIGURE 9. Ouest. The projected total *symptomatic* individuals, vs. time. Circles - observed; solid line - model prediction; Dashed lines - 5, 50, and 95 percentiles for model projections based on past 13 years precipitation records. Red lines are model runs with vaccination schedule that occurred in Spring 2012 (see text). The slow down in growth in late February and March was before the vaccination program began.

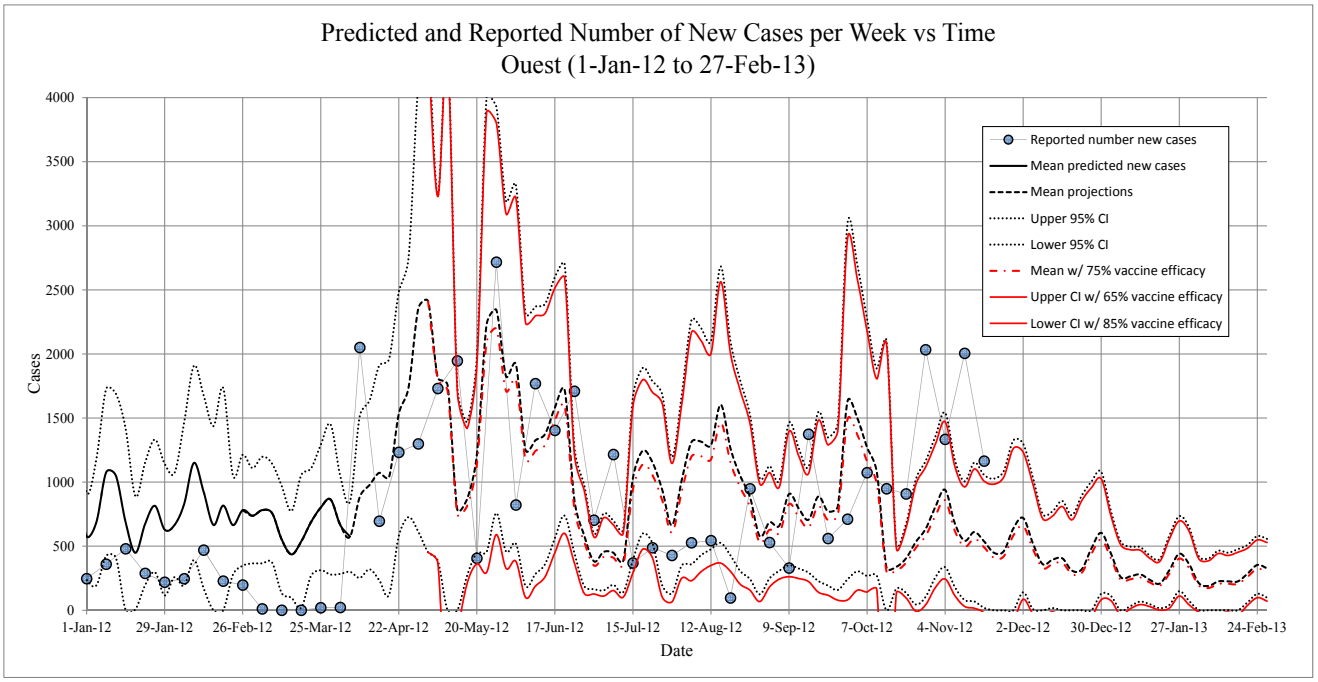

FIGURE 10. Ouest. The projected new *symptomatic* individuals, vs. time. Circles - observed; solid line - model prediction; Dashed lines - 5, 50, and 95 percentiles for model projections based on past 13 years precipitation records.

4. Discussion

Use of environmental data to model the dynamics of cholera in Haiti has been hampered by the lack of historical records. We use NASA satellite data to address this problem. This study shows that with environmental data of sufficient detail and quality, projections of disease progression can be made with sufficient lead time to prepare for outbreaks. The lag times of over five weeks means that if even rudimentary but reliable meteorological and coastal records are kept, preparations and resources can be more focused. The gathering of basic weather information is simple and inexpensive and should be made standard procedure when any agency takes part in interventions, particularly when the environmental component of the epidemiology is so well established.

In addition we explored the hypothesis that, at least in the Ouest region, tidal influences play a significant role in the dynamics of the disease. It appeared that tidal range rather than the height of the tide itself had the strongest influence. Some connection to tidal influences should be expected where large populations are in close contact with bays and estuaries, and humans are consuming local seafood.[17,28]

We also affirmed the longer time lags (8 - 10 weeks) found in previous studies from Africa[16] and shorter ones (4 weeks) in Bangladesh.[17]

Over the course of the epidemic the incidence has been tapering off. There has been steady and continued effort to improve hygiene and living conditions, however, the areas where the greatest strides are made are those where people leave the camps to return to normal living conditions and employment. The declining numbers of those at risk in the overall population belie the fact that many local populations are still without basic hygienic facilities. This was reflected in the model by setting a level u_0 to 5% of the original number of susceptible. This value matches the approximate 5% of the population that still remain displaced after the 2010 earthquake.[27]

On top of predicting when and how many cholera cases will rise with Haiti's climate and tides, any modeling to predict the effectiveness of interventions (such as vaccination) should consider these patterns. Considering that cholera may be maintained in the environment outside the human chain of infection is essential to planing effective prophylaxes and interventions.

Using these models we were able to assess, to some degree, the relative effectiveness of the recent vaccination program in Artibonite and Ouest. The discrepancy between the apparent effectiveness of vaccination in the two regions is perhaps not that puzzling when one considers the number vaccinated relative to the size of at risk population. In Artibonite about 41 thousand people and in Ouest about 47 thousand people received both doses of the vaccine. However, our model suggests that in Artibonite the at risk population by 6-May was about 61 thousand whereas in Ouest it was still over 428 thousand, seven times the number in Artibonite. Thus in Artibonite 67% of the most at risk population apparently received the vaccine, while in Ouest only 11% did. Further, in both regions 100 people receiving vaccination does not mean 100 people protected. The vaccine is about 75% effective,and only 21% of

people who are infected with cholera show symptoms, $0.75 \times 0.21 = 0.1575$. So as a rough calculation we might expect $0.1575 \times 41,000 = 6457.5$ and $0.1575 \times 47,000 = 7402.5$ people protected directly and additional due to the reduction in environmental loading of cholera bacteria and the force of infection. Ultimately, more people will be protected in Ouest but it will take longer to become apparent due to this dilution effect.

4.1. **Conclusion.** Although progress has been made in the past two years in modeling the Haitian cholera epidemic, only one model, so far, has accounted for seasonal variation due to precipitation, and none have examined temperature or tidal influences. Our paper shows that with basic climatic and tidal records and a relatively unsophisticated modeling procedure, not only can these factors be accounted for but also the time lags between climatic events and outbreaks can be identified. This approach looks at specific climatic events on the scale of a week rather than just seasonal patterns. We use daily tidal range as a predictive factor for cholera epidemics for the first time in a modeling paper, and we use real time daily precipitation estimates. These provide a level of detail of environmental events in conjunction with the lag times and estimates of core population size that can help evaluate intervention (such as vaccination) and public hygiene efforts. In order to show this we examined recent vaccination efforts in the Haitian cholera epidemic. Complex environmental patterns incorporated in epidemic models allow us remove a large source of variability and bring into relief intervention efforts by identifying deviations from the current.

5. Acknowledgements

Thanks to Scott Braun and George Huffman at NASA, Goddard Space Flight Center for help accessing precipitation data.

Thanks to Scott Dowell and Jordan Tappero at CDC; Louise Ivers at PIH; and Jean Pape at GHESKIO for information about the cholera vaccination programs in Haiti.

This project was partially supported by a CCFF grant of the Columbian College of Arts and Sciences, of The George Washington University. S.R. was also partially supported by the NSF CAREER grant #1151618.

References

[1] World Health Organization. (2012) WHO|Haiti. (http://www.who.int/hac/crises/hti/en/). Accessed 28 April 2012.

[2] Cravioto, A, Lanata, C. F, Lantagne, D. S, & Nair, G. B. (2011) Final report of the independent panel of experts on the cholera outbreak in haiti., (United Nations), Technical report. Retrieved from http://www.un.org/News/dh/infocus/haiti/UN-cholera-report-final.pdf.

[3] Piarroux, R, Barrais, R, Faucher, B, Haus, R, Piarroux, M, Gaudart, J, Magloire, R, & Raoult, D. (2011) Understanding the cholera epidemic, Haiti. *Emerg Infect Dis* **17**, 1161–1168.

[4] Ministère de la Santé Publique et de la Population. (2012) Daily reports of mspp on the evolution of cholera in haiti., (Republique d'Haiti), Technical report. Retrieved from http://www.mspp.gouv.ht/site/index.php?option=com_content&view=article&id=120&Itemid=1.

[5] Knox, R. (2012) Shots: NPR's health blog. Port-au-Prince: A city of millions, with no sewer system. (http://www.npr.org/blogs/health/2012/04/13/150501695/port-au-prince-a-city-of-millions-with-no-sewer-system?ps=sh_sthdl). Accessed 2 May 2012.

[6] Pan American Health Organization. (2012) Interactive atlas of the cholera outbreak in la Hispaniola, 2010-2012. (http://new.paho.org/hq/images/Atlas_IHR/CholeraHispaniola/atlas.html). Accessed 3 March 2012.

[7] Andrews, J. R & Basu, S. (2011) Transmission dynamics and control of cholera in Haiti: an epidemic model. *Lancet* **377**, 1248–1255.

[8] Tuite, A. R, Tien, J, Eisenberg, M, Earn, D. J, Ma, J, & Fisman, D. N. (2011) Cholera epidemic in Haiti, 2010: Using a transmission model to explain spatial spread of disease and identify optimal control interventions. *Annals of Internal Medicine* **154**, 593–601.

[9] Bertuzzo, E, Mari, L, Righetto, L, Gatto, M, Casagrandi, R, Blokesch, M, Rodriguez-Iturbe, I, & Rinaldo, A. (2011) Prediction of the spatial evolution and effects of control measures for the unfolding Haiti cholera outbreak. *Geophysical Research Letters* **38**, L06403.

[10] Chao, D. L, Halloran, M. E, & Longini, Jr., I. M. (2011) Vaccination strategies for epidemic cholera in haiti with implications for the developing world. *Proceedings of the National Academy of Sciences* **108**, 70817085.

[11] Codeço, C. T. (2001) Endemic and epidemic dynamics of cholera: the role of the aquatic reservoir. *BMC Infectious Diseases* **1**, 1–14.

[12] Reiner, Jr., R. C, King, A. A, Emch, M, Yunus, M, Faruque, A. S. G, & Pascual, M. (2012) Highly localized sensitivity to climate forcing drives endemic cholera in a megacity. *Proceedings of the National Academy of Sciences* **109**, 20332036.

[13] Rinaldo, A, Bertuzzo, E, Mari, L, Righetto, L, Blokesch, M, Gatto, M, Casagrandi, R, Murray, M, Vesenbeckh, S. M, & Rodriguez-Iturbe, I. (2012) Reassessment of the 20102011 haiti cholera outbreak and rainfall-driven multiseason projections. *Proceedings of the National Academy of Sciences* **109**, 66026607.

[14] Knox, R. (2012) Shots: NPR's health blog. vaccination against cholera finally begins in Haiti. (http://www.npr.org/blogs/health/2012/04/12/150493770/vaccination-against-cholera-finally-begins-in-haiti?ps=sh_sthdl). Accessed 2 May 2012.

[15] United Nations. (2012) Haiti|reliefweb. (http://reliefweb.int/country/hti).

[16] Reyburn, R, Kim, D. R, Emch, A, Khatib, A, von Seidlein, L, & Ali, M. (2011) Climate variability and the outbreaks of cholera in Zanzibar, East Africa: A time series analysis. *The American Journal of Tropical Medicine and Hygiene* **84**, 862–869.

[17] de Magny, G. C, Murtugudde, R, Sapiano, M. R. P, Nizam, A, Brown, C. W, Busalacchi, A. J, Yunus, M, Nair, G. B, Gil, A. I, Lanata, C. F, Calkins, J, Manna, B, Rajendran, K, Bhattacharya, M. K, Huq, A, Sack, R. B, & Colwell, R. R. (2008) Environmental signatures associated with cholera epidemics. *Proceedings of the National Academy of Sciences* **105**, 17676–17681.

[18] Koelle, K, Rodó, X, Pascual, M, Yunus, M, & Mostafa., G. (2005) Refractory periods and climate forcing in cholera dynamics. *Nature* **436**, 696–700.

[19] Tien, J. H & Earn, D. J. D. (2010) Multiple transmission pathways and disease dynamics in a waterborne pathogen model. *Bulletin of Mathematical Biology* **72**, 1506–1533.

[20] Neilan, R. L. M, Schaefer, E, Gaff, H, Fister, K. R, & Lenhart, S. (2010) Modeling optimal intervention strategies for cholera. *Bulletin of Mathematical Biology* **72**, 2004–2018.

[21] Hartley, D. M, Morris, Jr., J. G, & Smith, D. L. (2006) Hyperinfectivity: A critical element in the ability of *V. cholerae* to cause epidemics? *PLoS Med* **3**, e7.

[22] NASA. (2012) NASA earth data. daily TRMM and other satellites precipitation product (3B42 V7 derived) (TRMM_3B42_daily). (`http://mirador.gsfc.nasa.gov/cgi-bin/mirador/` [data files]). Accessed June 2012.

[23] The Weather Underground. (2012) Mean temperature (and other) weather history for Port-au-Prince, Haiti. (`http://www.wunderground.com/history/airport/MTPP/2012/1/1/CustomHistory.html`). Accessed 11 June 2012.

[24] NOAA. (2012) NOAA tides & currents website: Tide predictions - application. (`http://tidesandcurrents.noaa.gov/noaatidepredictions/NOAATidesFacade.jsp?Stationid=TEC4709`). Accessed 25 June 2012.

[25] Ramsay, J, Hooker, G, Campbell, D, & Cao., J. (2007) Parameter estimation for differential equations: a generalized smoothing approach. *Journal of the Royal Statistical Society: Series B (Statistical Methodology)* **69**, 741–796.

[26] Kaper, J. B, Morris, Jr., J. G, & Levine, M. M. (1995) Cholera. *Clinical Microbiology Reviews* **8**, 48–86.

[27] CERF (Office for the Coordination of Humanitarian Affairs - United Nations). (2012) CERF gives $8 million to support humanitarian activities in haiti. (`http://ochaonline.un.org/CERFaroundtheWorld/Haiti2012/tabid/7810/language/en-US/Default.aspx`). Accessed 10 July 2012.

[28] Huq, A, Small, E. B, West, P. A, Huq, M. I, Rahman, R, & Colwell, R. R. (1983) Ecological relantionships between *Vibrio cholerae* and planktonic crustacean copepods. *Applied and Environmental Microbiology* **45**, 275–283.

[29] Date, K. A, Vicari, A, Hyde, T, Mintz, E, Danovaro-Holliday, M. C, Henry, A, & et al. (2011) Considerations for oral cholera vaccine use during outbreak after earthquake in haiti, 2010-2011. *Emerg. Infect. Dis.* **17**, 2105–2112.